Edge-Assisted Control for Healthcare Internet-of-Things: A Case Study on PPG-based Early Warning Score

ARMAN ANZANPOUR, University of Turku, Finland
DELARAM AMIRI, University of California, Irvine, USA
IMAN AZIMI, University of Turku, Finland
MARCO LEVORATO, University of California, Irvine, USA
NIKIL DUTT, University of California, Irvine, USA
PASI LILJEBERG, University of Turku, Finland
AMIR M. RAHMANI, University of California, Irvine, USA

Recent advances in pervasive Internet of Things (IoT) technologies and edge computing have opened new avenues for development of ubiquitous health monitoring applications. Delivering an acceptable level of usability and accuracy for these healthcare IoT applications requires optimization of both *system-driven* and *data-driven* aspects, which are typically done in a disjoint manner. While decoupled optimization of these processes yields local optima at each level, synergistic coupling of the system and data levels can lead to a holistic solution opening new opportunities for optimization. In this paper, we present an edge-assisted resource manager that dynamically controls the fidelity and duration of sensing w.r.t. changes in the patient's activity and health state, thus fine-tuning the trade-off between energy-efficiency and measurement accuracy. The cornerstone of our proposed solution is an intelligent low-latency real-time controller implemented at the edge layer that detects abnormalities in the patient's condition and accordingly adjusts the sensing parameters of a reconfigurable wireless sensor node. We assess the efficiency of our proposed system via a case study of PPG-based medical Early Warning Score (EWS) system. Our experiments on a real full hardware-software EWS system reveal up to 49% power savings while maintaining the accuracy of the sensory data.

Additional Key Words and Phrases: Health Monitoring, Wearable Electronics, Early Warning Score, Internet of Things, Edge Computing, Edge-Assisted Control

1 INTRODUCTION

Remote health monitoring is expected to fundamentally transform many healthcare applications to be used in everyday settings. Beyond the use of health monitoring systems for general health reports, these systems can predict and prevent deterioration and death in chronic patients [77]. Such applications demand a satisfactory level of quality, which poses tremendous challenges in the face of real-time and personalized health monitoring systems. A key mechanism to manage and implement such applications is leveraging pervasive Internet of Things (IoT) technologies [53, 64].

In the most prevalent IoT architecture, smart objects interchange their data with remote servers through a gateway so that the processing resources are mostly concentrated on the server side. In healthcare applications, utilizing such fully centralized processing methods puts the continuity of remote patient monitoring services at the risk of failure. Edge (i.e., Fog) computing is a method for extending the compute, storage, and network facilities to the edge of the network by outsourcing the tasks needing low-latency and real-time support [5].

Edge computing not only provides local notification, processing, and storage but also reduces the data traffic through data fusion. Moreover, the lower radio signal strength required for wireless data transmission in shorter ranges reduces the sensor node power consumption significantly [56, 57].

2020. XXXX-XXXX/2020/7-ART1 $15.00
DOI: 10.1145/nnnnnnn.nnnnnnn

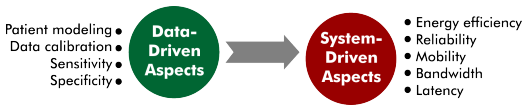

Fig. 1. Coupling system-driven and data-driven approaches

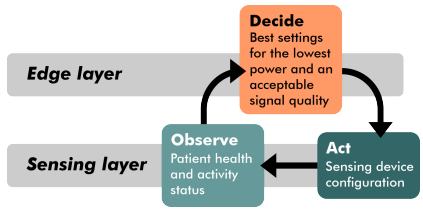

Fig. 2. ODA system control loop

There is a high demand to enhance the quality of experience in healthcare IoT applications adaptively, generally from two different often disjoint aspects: *system-driven* and *data-driven* (see Figure 1). There are several studies [63, 69, 76] on optimizing system-driven aspects by leveraging cognition to enhance single or multiple system characteristics; however, these efforts are in fact agnostic to the content and semantics of the transmitted data. For instance, consider a remote healthcare monitoring application, where the health condition of an at-risk patient is transitioned between "normal" to "abnormal". Here, these semantics (from the data-driven aspects) allow us to properly adjust the sensing settings and sensing duration (in the system-driven aspects). Therefore, the system-driven parameters (e.g., energy and bandwidth) can be optimized considering the requirements of "normal" and "abnormal" states without loss of significant information.

With the prevalence of IoT-base remote patient monitoring, a vast number of medical conditions are trackable, and most of their complications are preventable. Specifically, in chronic diseases, which are the leading cause of death and disability worldwide, the emergency situation precedes with a sudden deterioration. It has been shown that the early signs of such deterioration are observable in the patient vital signs several hours earlier [39, 41, 42], and preventing the deterioration reduces the risk of death [75]. Monitoring the vital signs of a chronic patient remotely enables the detection of a potential deterioration and prevention of death or disability. However, the main issue here is due to patient daily activities out of the hospital, which affects the quality of the recorded signals [3].

In this paper, we propose an edge-assisted solution that makes the sensing, processing, and configuration of the IoT system cognitive and self-aware. The system is capable of adapting its sensing energy and signal quality parameters to the patient's activity and health status, which are defined as system context. The context-aware solution we propose to preserve the quality of biosignals for an active subject is set based on an ODA loop (*Observe*, *Decide*, *Act*). In an ODA system control loop (Figure 2) the process of *Observation* examines the current status of the system, the *Decision* process decides how to control the system according to observations, and the *Action* process applies the results of decision making on the system. The *Decision* that comes to *Action* according to *Observations* on the involved system layers provides the system with a level of context-awareness. In our solution, the observation and act processes happen on the sensing layer and the decision-making which is the main contribution of our work happens on the edge. *Observation* includes the assessment of the patient activity and health status, the *Decision* is the lowest power state of the signal recording device while targeting an acceptable level of quality, and the *Action* is a configuration command for sensing device defined in the *Decision* process. We chose edge computing because it is the most efficient IoT architecture to implement our idea without imposing any computation overhead to the sensor layer while offering rapid response at the edge. In the healthcare domain, highly reliable services are needed which can be served more consistently and promptly when the decision-making core is closer to the patient. The *Action* process is faster with edge computing, and the risk of network failure is minimum.

The main novelty of our solution is i) a decision-making method which leverages both the physical activity and health status of the patient (via Early Warning Score method) to decide the required actuation on the sensor node, and ii) a cross-layer control mechanism in which the application/data layer informs the system layer when opportunistic energy-savings would be feasible while preserving the accuracy of sensing.

In this work, we also present a real use case of our system via a Photoplethysmograph (PPG) sensor-based case study on Early Warning Score (EWS). EWS is a risk scoring method designed for early detection of possible health deterioration using the patient's vital signs [45].

The contributions of this paper are the following:

- We design an edge-based remote health monitoring architecture and a reconfigurable sensor node for Early Warning Score (EWS) assessment in out-of-hospital settings.
- We assess the error/noise resiliency of feature extraction in the bio-signals for varying sensing energy consumption and a person's activity.
- We formulate an optimization problem to minimize the long-term energy consumption of a sensor node for a given target accuracy of extracted parameters.
- We develop a run-time control algorithm state machine residing at the edge layer to enable the real-time adaptation of the sensing parameters to patients' states.
- We evaluate our proposed system in terms of accuracy and energy consumption of the sensing layer for an EWS case-study where a user engages in various physical activities during daily routine.

The rest of the paper is organized as follow: In Section 2, we introduce essential concepts as a background. Section 3 outlines related works. The proposed healthcare IoT system is presented in Section 4. Section 5 demonstrates and evaluates the system performance, and Section 6 concludes the work.

2 BACKGROUND

The development of an edge-assisted remote health monitoring system through a context-based optimization solution needs knowledge about patient health status [4, 46]. Therefore, a reliable health indicator is required to find abnormalities. Here, we use the Early Warning Score (EWS) for this purpose, which similar to most health indicators, relays on the changes in the vital signs. To make a compact and wearable sensing device, we choose the PPG sensor as a source for most of the vital signs. PPG signal is a rich source of medical information but very sensitive to patient activities. In this section, we briefly introduce the Early Warning Score (EWS) and Photoplethysmography (PPG) methods. Moreover, we outline the limitations of PPG and our methods for vital signs and activity detection.

2.1 Early Warning Score (EWS)

Studies show that health deterioration detection within a short time frame plays a crucial role in patients' survival [52, 68]. There is solid evidence that such deterioration is distinguishable in patients' vital signs several hours prior to adverse medical events.[65] Thus far, several risk score methods have been proposed to track the vital signs manually and notify such events earlier.[15] Early Warning Score (EWS) proposed by Morgan *et al.* [45] is a tool for detecting the early signs of health deterioration in order to prevent ICU admission. This method is an instruction for recording and comparing patient vital signs (i.e., heart rate, blood pressure, respiration rate, body temperature, blood oxygen saturation, and level of consciousness) to determine the severity of sickness. Based on the observation of certain vital signs, EWS calculates a score for each vital sign where the sum

Table 1. A conventional Early Warning Scores (EWS) chart [73]

Score	3	2	1	0	1	2	3
Heart rate[1]	0-39	40-50	51-59	60-100	101-110	111-129	130+
Systolic BP[2]	0-69	70-80	81-100	101-149	150-169	170-179	180+
Respiratory rate[3]		0-8		9-14	15-20	21-29	30+
Body temperature[4]		0-35		35.1-38		38.1-39.5	39.6+
SpO2 (%)	0-84	85-89	90-94	95-100			
Level of consciousness				Alert	Reacting to voice	Reacting to pain	Unresponsive

[1]beats per minute, [2]mmHg, [3]breaths per minute, [4] °C

of all individual scores shows the degree of abnormality. Table 1 indicates a conventional early warning score [45].

EWS is used in hospitals as a guideline for the track-and-trigger system, which updates the number of patient's observations per hour when the medical team is alerted in case of high scores. The standard EWS scoring ranges for each vital sign are defined for a patient in a hospital setting. However, in everyday settings, the activity and environment affect these limits and scores. In this paper, we use a modified self-aware early warning score, which provides a scale for patient health status considering the patient's activity and environment [9, 11, 25]. For this purpose, a patient's activities should also be recorded together with standard vital signs.

2.2 Photoplethysmograph (PPG)

Photoplethysmograph (PPG) is an optical technique representing blood volume variations in the microvascular [28] from which vital signs, including heart rate, respiration rate, and blood oxygen saturation can be obtained. PPG measurement can be performed using a non-invasive and low-cost miniaturized sensor. For this reason, PPG sensors are widely integrated into portable medical and wearable sensors (e.g., fitness trackers, wristbands, smart watches) to continuously capture vital signs.

A PPG sensor consists of 1-2 single-wavelength light sources together with a light sensor in contact with a body organ containing microvascular end-points such as fingertip (Figure 4 (a)). This sensor measures the amount of light reflection or absorption by blood which depends on blood volume, light wavelength and the amount of oxygenated and deoxygenated hemoglobin molecules. Figure 4 (b) shows the differences in light absorption intensity for fully saturated (red line) and fully desaturated (blue line) hemoglobin molecules in two selected wavelengths. The ratio of light absorbance in these two sample wavelengths provides the value of blood oxygen saturation.

A PPG waveform reflects volumetric changes in the microvascular bed of tissues. Such a signal comprises two major components as alternating current (AC) and direct current (DC), whose changes are attributed to synchronous variations in the blood volume oscillating with heartbeat and respiration, respectively [2]. The heart beat and respiratory oscillations in a PPG signal are indicated in Figure 5.

Recent works show that in addition to the above data, several other procedures, such as continuous measurement of finger arterial blood pressure, cardiac output measurement, and vascular assessments are also possible via continuous PPG signal monitoring [12, 32].

2.3 PPG Limitations

Despite many benefits of using the PPG method for collecting vital signs, there are also some limitations utilizing this method. The main drawback of the PPG method is its high power consumption compared to other medical sensors. While the power consumption of ECG, respiration,

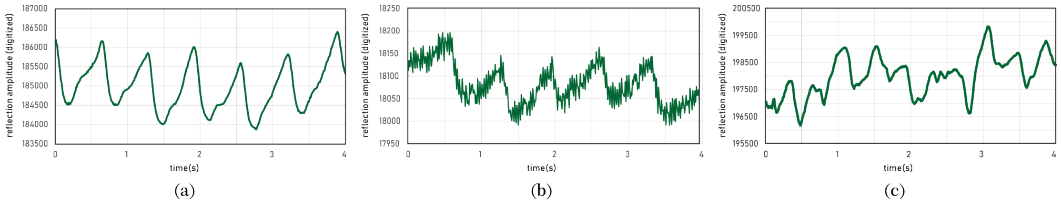

Fig. 3. PPG signal quality samples collected from finger tip: (a) high-current, sleeping (b) low-current, sleeping (c) high-current, running

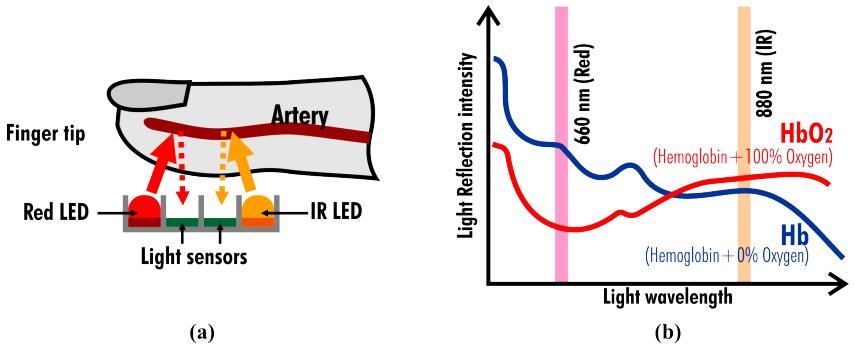

Fig. 4. (a) PPG sensors including two light sources and two light sensors (b) Light absorption intensity for fully saturated and fully desaturated hemoglobin molecules [23, 34]

and temperature sensors are in the range of microWatt, the power consumption of most PPG sensors are in the range of milliWatt and without power management policies, the application of this sensor in wearables would be minimal. PPG sensor has one or two light-emitting diodes (LED) which turning them on draws 1 to 10 mA current. While applying higher currents makes the LEDs brighter and leads to higher signal quality, in lower currents, the ambient light interferes with the sensing process and makes a noisy signal.

The other drawback of the PPG signal is its vulnerability to body movements. Body movements change the shape of blood vessels and surrounding tissues and make rapid changes in the DC part of the signal. The noisy signals due to activities and low power measurements lead to low-accuracy vital signs. [47] *As mentioned earlier in section 1, the main contribution of this study is an edge-assisted control that manages the power consumption of a PPG-based sensor node while keeping the signal noise (and therefore the accuracy of vital signs) in an acceptable range.* Figure 3 shows the effect of applying current and activity on the PPG signal.

2.4 Bio-signals Extraction

Thus far, several methods have been proposed to extract respiration rate and heart rate signals from the raw PPG waveform [17, 54]. For the respiration rate, there are two major methods to obtain the signal named as feature-based and filter-based techniques.

In the feature-based techniques, specific features (e.g., maximum intensity of the pulse and baseline variations) are extracted to provide respiration rate values [33]. However, these methods are insufficient for our system because the features cannot be obtained due to the effect of ambient and motion noise on the signal. Such sources of noise are inevitable in ubiquitous health monitoring, as users might engage in various physical activities in different environments.

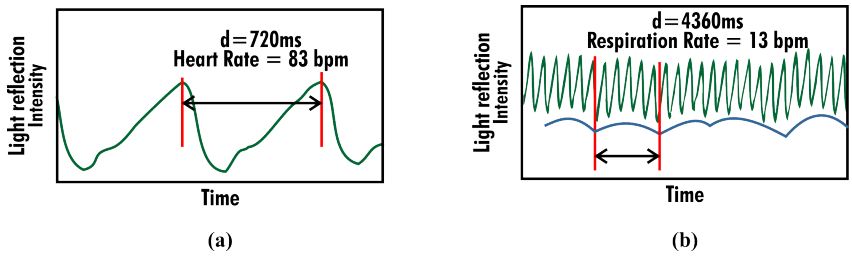

Fig. 5. Oscillations reflected in a PPG signal. (a) heart rate. (b) respiration rate.

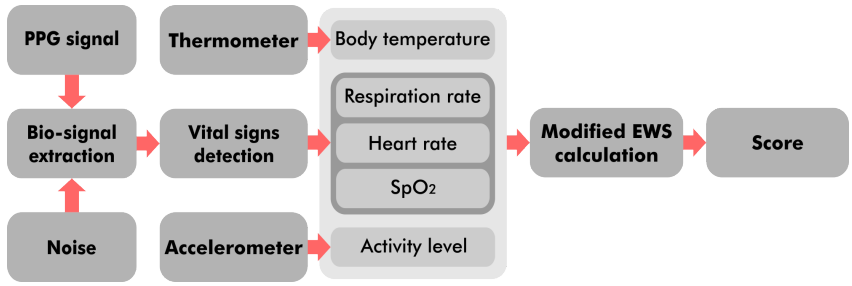

Fig. 6. Modified EWS calculation using PPG, temperature and acceleration signals

On the other hand, the respiration rate is obtained via filter-based techniques, where certain band-pass filters are designed to discard non-respiratory frequency domain [21]. Correspondingly, such filters can be designed for heart rate extraction.

In our system, a filter-based technique is tailored to mitigate the impact of motion artifacts on the outcome. In this regard, two band-pass filters are designed according to the respiration rate and heart rate frequency domains. The respiration and heartbeat frequency ranges are generally limited to 0.1-1 Hz (6-60 breath rate/minute) and 0.5-3.0 Hz (30-180 heart rate/minute). The boundaries can be chosen for the filters' cutoff frequency, although such a selection method might be inappropriate when the user is moving, because the pass frequency is too wide. Hence, the filter's pass frequency needs to be precisely selected w.r.t. the current situation.

In this regard, a filter's cut off frequency selection is extemporaneously performed exploiting the peak values in the power spectral density (PSD) of the incoming PPG signal [38]. Figure 7 clearly illustrates frequency peaks corresponding to respiration and heartbeat oscillations in the PSD of a one-minute PPG signal collected from a healthy person while he is sleeping. Heartbeat signal is extracted using the peak value in the heart rate frequency range. As shown in the figure, respiration frequency range might hold the heart rate peak as well. Since the heartbeat signal is first discarded, the peak value in the respiration frequency range reflects the respiration signal. Note that a high noise level nevertheless alters the structure of the PSD of the signal and subsequently hinders the bio-signals extraction. Therefore, an adequate signal-to-noise ratio (SNR) is required in this approach. Using this property, we can opportunistically adjust the sensing energy (i.e., the power used by the sensor to emit/capture IR and red signals) depending on the current state of the user,—e.g., "jogging" state leads to a low SNR, therefore a high sensing energy is needed to enhance the signal, while "Sleeping" state results in a high SNR which demands a low sensing energy.

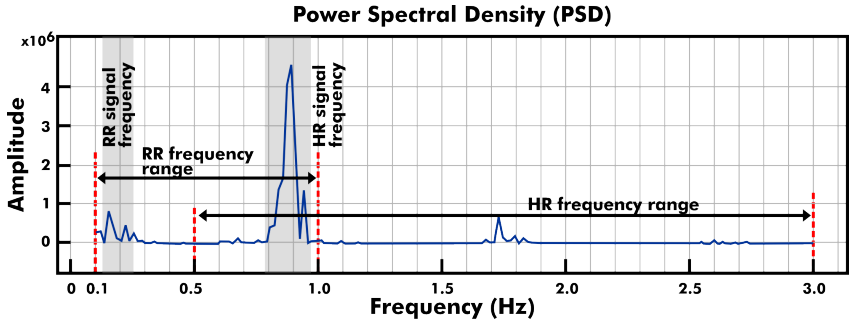

Fig. 7. The power spectral density of a one-minute PPG signal

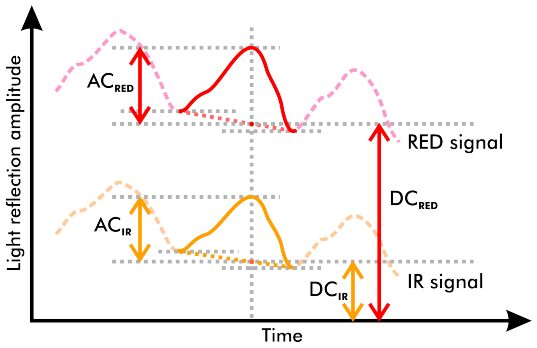

Fig. 8. The alternative currents and direct currents of the IR and red signals to retrieve SpO_2

2.5 Vital Signs Detection

In our system, we exploit a peak detection method in which both heart rate and respiration rate are differentiated. The average time interval between consecutive local maxima in the derivative signals indicates the heart rate and respiration rate values.

Despite the aforementioned detection algorithm, we determine the SpO_2 value via a feature-based method, where four features are extracted: the alternative currents and direct currents of the IR and red signals (i.e., AC_{IR}, AC_{RED}, DC_{IR} and DC_{RED}) (see Figure 8). The SpO_2 is determined using the following equations:

$$R = \frac{AC_{RED}.DC_{IR}}{AC_{IR}.DC_{RED}} \tag{1}$$

$$SpO_2 = \alpha R^2 + \beta R + \gamma \tag{2}$$

where α, β and γ are constants retrieved from the sensor's specification [31].

As indicated in Table 1, various vital signs are required to provide the warning score for users. We use PPG signals to extract three of the vital signs. A temperature sensor is also used to measure body temperature. Eventually, a modified warning score is calculated leveraging the four vital signs along with physical activity data. Since patient deterioration is mainly caused by respiration inefficiency and lack of enough oxygen intake [40], and due to non-continuous nature of blood pressure monitoring, the blood pressure is excluded from this setup. Figure 6 illustrates the schema of the score calculation process.

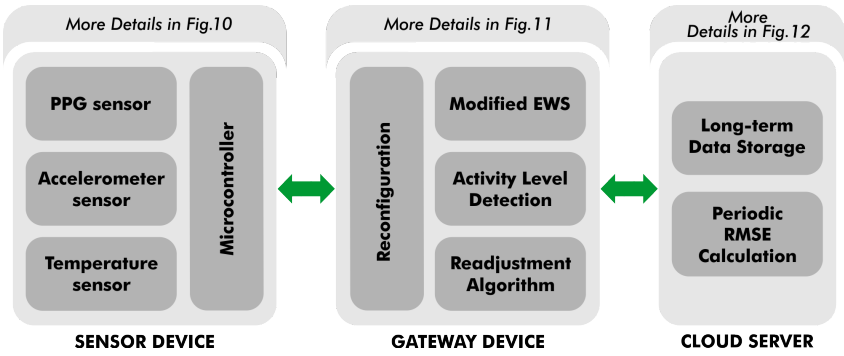

Fig. 9. The three-layer architecture of the proposed system

2.6 Physical Activity Recognition

In our work, the 3D acceleration data is utilized to determine the user's physical activity continuously. As the accelerometer sensor is placed at the user's hand, we use hand movements to extract the user's steps. In this regard, first, the acceleration data is filtered, mitigating the ambient noise. Then, walking cycles are extracted from the data via a peak detection algorithm. Subsequently, the steps are counted at each time interval. When the user is still (i.e., no step is detected) the orientation of the user is leveraged to specify whether the current activity is sleeping or sitting.

In our setup, we use the steps and orientation data to determine a physical activity for each time interval. The physical activities are "sleeping", "sitting", "walking", "jogging" (i.e., moderate activity) and "running" (i.e., vigorous activity) [71, 72].

2.7 Modified EWS Calculation

The extracted vital signs are used in EWS calculation. As mentioned in Section 2.1, the conventional EWS method is inappropriate for out-of-hospital setting, therefore we leverage a modified EWS method proposed in [9, 11] where context data (e.g., physical activities) are also considered in the calculations. In such a method, the score ranges (Table 1) are dynamically fine-tuned according to the user's situations. This adjustment is performed via a pre-defined rule-based algorithm, in which meta-data (e.g., user's feedback) could also be added throughout the monitoring to deliver a personalized decision making.

3 RELATED WORKS

The development of this research benefits from several concepts and technologies. The main objective of this study is to design an architecture for remote health monitoring, which satisfies users' needs with a minimum level of quality in every situation. Since an increase in physical activity level decreases the signal-to-noise ratio for most medical signals, we reconfigure the parameters of the sensing device according to the subject's activity level and health status to keep the quality of signal in an acceptable range. Such reconfigurations are applicable for a signal which: a) is prone to noise during the activity b) has an adjustable knob which feeds more resources to the system to provide a less noisy signal. Among medical signals, ECG, EMG, GSR, and PPG signals have these characteristics. Since the patient's health status is also an essential factor in reconfiguration, we use the EWS method for health assessment and because the EWS requires the vital signs, we choose PPG signal which has a compact sensor and can alone provide three vital signs. To make the monitoring remotely possible, we leverage an IoT-based architecture for data

collection and to be able to respond to patient state fast, we process the data on the fog layer. To analyze the incoming data and make the most right configuration for the sensor, we optimize the activity/accuracy problem during design-time and run-time. To the best of our knowledge, the proposed architecture is not described in the literature yet, but in each of the mentioned sections it has several related works that we summarize them here.

Edge computing is defined as methods for relocating the processing load and network resources from traditional cloud servers to local gateways [13, 61]. The aim of these methods is to offload compute-intensive tasks to the edge devices to save energy [18, 19, 37, 55], reduce the response latency by avoiding massive data transmission to the cloud [14, 26, 30, 59], and reduce the bandwidth by data preprocessing [30]. Several works also present the benefits of fog-assisted remote reconfiguration of sensor nodes [29, 36, 48, 50]. However, these solutions solely focus on the data processing aspect, without an in-depth exploitation of edge devices to perform system optimization through a closed-loop low-latency local control.

Some recent efforts have attempted to provide a degree of adaptivity to enable efficient IoT services. Several frameworks have been proposed for bringing intelligence to IoT-enabled solutions via architectural designs [76], energy management [69], object virtualization [60], and protocol design [1]. Most of these works develop intelligence to optimize and control the device layer at a user-state agnostic level. Our work presents a cognitive model that provides a system-user tightly-coupled control of the data sensing and transmission processes by considering the state of the user obtained from the same process.

Power consumption reduction techniques in sensor nodes have been proposed earlier using different methods such as powering off sensors and radio transmission modules to reduce the power consumed by those parts [22, 74], reducing local processings [6], reducing data transmission[67], and turning processing units to sleep or deep sleep modes[44].

Different schemes have been introduced to optimize the energy efficiency of sensor network while detecting the activities of an individual. Partially observable Markov decision process (POMDP) frameworks are proposed in [78] and [80] to detect one's activity based on noisy measurements of mean and variance values of an accelerometer sensor and period of an ECG sensor using a Kalman filter estimator. Optimization of an individual's physical activity detection while minimizing the energy consumption of wireless networks is proposed in [79]. However, Zois *et al.* [79] assume that the energy bottleneck is at the gateway level rather than the sensor nodes, and reducing the signal quality while maintaining a minimum level of accuracy has not been considered in these solutions. These works have applied their power consumption reduction solution on the sensing or the gateway device completely independent from the user's health, while in our proposed method, not only we set sensor node configurations according to user activity status, but also we pay attention to his/her health status.

Most of the proposed sensor control solutions focus either on the quality of data (which we consider it as data-driven aspects) or the efficiency of the power consumption in the system (which we name it system-driven aspects) and those few works that managed to couple these two aspects, the optimization target has not been in the sensing layer. Our formulation in this paper is based on the assumption that sensors are energy-constrained and their accuracy is a function of the user-state (i.e., activity) and can be controlled at run-time.

Moreover, there are several solutions for IoT-based health monitoring [7, 8], measuring the accuracy of wearable health monitors [27, 49, 58], investigating the effect of activity on the accuracy of health signals [43, 78–80], assessment the effect of environmental parameters on the quality of PPG signal [16, 20, 70], and adjusting the power consumption of a wearable medical device via self-awareness [9], context-awareness [24], and goal management methods [10], but none of them

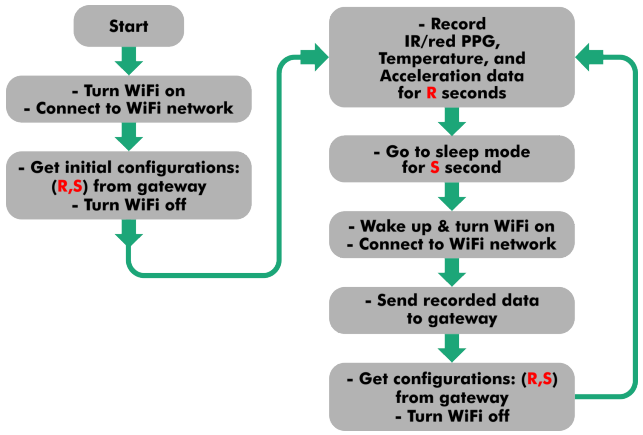

Fig. 10. Sensor device functions flowchart

has proposed a solution for configuring a sensing device in a fog-assisted control loop to optimize the power consumption while preserving the quality of data in an acceptable level.

4 THE PROPOSED HEALTHCARE IOT SYSTEM

The proposed system architecture consists of three layers: the sensing layer, edge layer, and cloud layer.

In the first layer, reconfigurable sensing devices collect medical and activity data and send them to smart gateways in the edge layer. In reply, the gateways send a new configuration instruction to the sensors after evaluating the state of the user as well as the system. They also forward the aggregated user data to the cloud. The cloud stores the patient information in a database for long-term evaluations. Based on the stored data, the cloud updates the baseline parameters used in our edge controller at regular intervals. Figure 9 shows the three-layer architecture of the proposed system.

4.1 Reconfigurable Sensor Node

To leverage the local control feature provided by the edge layer, we propose a reconfigurable sensor node whose sensing fidelity and hibernate duration can be changed at run-time. The reconfigurable sensor node is a remotely programmable data collector that receives a command from the smart gateway regarding its new task in every iteration. In this work, our sensor node is a wireless activity and medical vital signs data recorder. It uses a PPG sensor for recording the light reflection intensities from the fingertip, a temperature sensor for measuring the skin temperature, and a 3D accelerometer for recording the patient's activities. A micro-controller communicates with these sensors and records collected data to a flash memory. After recording, the sensor node connects to the gateway using a low-power Wi-Fi module, transmits the recorded data to the edge layer, asks in reply for a new configuration command, and then goes to the hibernate mode for a time interval specified in the configuration. After hibernation duration, the sensor node wakes up and starts recording again according to the latest instruction. A web service in the gateway device receives, stores, and analyzes data and defines a new command for the sensor node according to the current patient's state. Figure 10 shows the details of the sensor device functions flowchart.

The configuration command contains instructions for defining record/hibernate duration and adjusting the power consumption of active sensor modules. The power consumption states of the

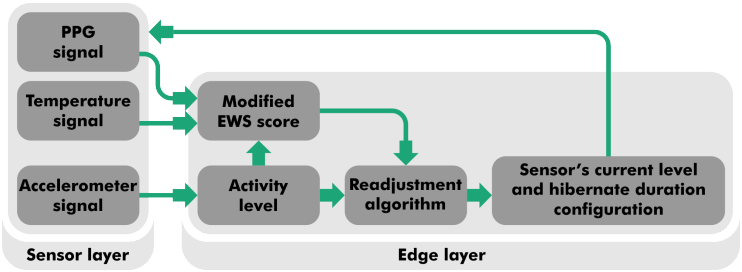

Fig. 11. High level Edge-assisted control architecture

sensor node are changed by turning off the radio communication during data recording and also by micro-controller hibernation. The power consumption of PPG sensor LEDs is also configurable and defines the recording sub-states.

4.2 Personalized Edge-assisted Controller

One of our design goals is to provide a high Quality of Experience (QoE) to IoT services and technologies. To this aim, we implement an edge-assisted controller interfaced with the sensing and processing layers of the system. We contend that the edge processor is in a unique position to bridge different scales of the system, enabling adaptation to local availability of resources and the state of the monitored person based on global information.

In the proposed architecture, the system includes a set of cognitive algorithms that observe and monitor states of the user to control sensing accuracy and duration and adapt the data acquisition process to the current context. For instance, when a patient is in the "Sleeping" state, the magnitude of motion artifacts is significantly lower than the "Jogging" state. Therefore, it demands a lower sensing energy to provide the same level of sensing accuracy (e.g., RMSE). Thus, activity-based sensing control can save a considerable amount of energy.

Figure 11 depicts an overview of the proposed edge-assisted control architecture for our target application. The self-aware cognitive engine at the edge layer optimizes the parameters of sensing and hibernation in response to the person's state. The objective is to maximize system's lifetime while maintaining a target detection accuracy from the PPG signal. The proposed optimization involves two interconnected aspects: *Sensing Fidelity* and *Sensing Duration*.

4.2.1 Sensing Fidelity. The system cognition consists of two phases, during which the edge determines the sensor current level based on the Root Mean Squared Error (RMSE) requirements:
i) Sensing Fidelity Design-time: In this phase, the edge processor builds a model connecting the control parameters to the overall accuracy. The PPG signal sent from the sensor is pre-processed and different features including, SpO_2, heart rate and respiration rate are extracted. Then, a set of reference signals (SpO_2, heart rate and respiration rate) are compared with the calculated features. Specifically, we use an ECG sensor as a reference for heart rate, an airflow sensor for respiration reference, and another PPG sensor with higher overall quality as a reference for SpO_2.

We compute the RMSE of the calculated features in the edge layer to be a function of both the current level, U and the activity state of the monitored person:
$X \in$ {Sleeping, Sitting, Walking, Jogging, Running}.

Varying the PPG sensor's current level U, we calculate the total RMSE as the weighted sum of the RMSE of the three individual features. The total error, then, is

$$\epsilon(U,X) = \{\gamma_1\epsilon_1(U,X) + \gamma_2\epsilon_2(U,X) + \gamma_3\epsilon_3(U,X)\}$$

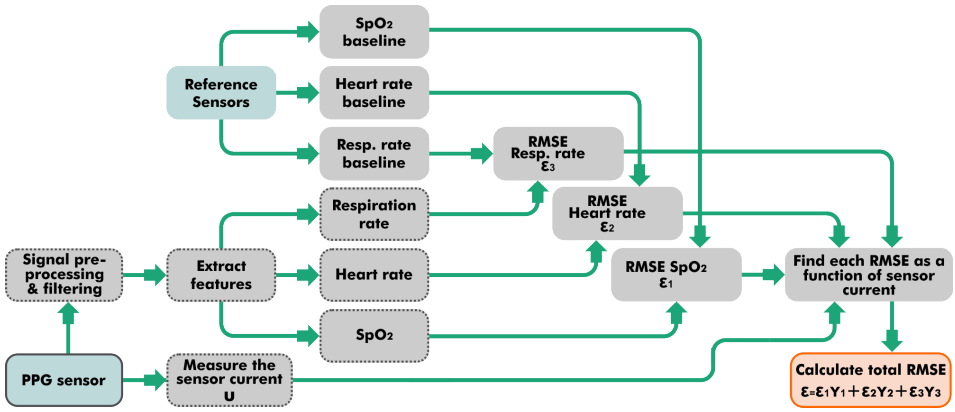

Fig. 12. System design-time block diagram

where $\epsilon_1(U,X)$, $\epsilon_2(U,X)$ and $\epsilon_3(U,X)$ are associated with heart rate, SpO_2 and respiration rate, respectively. Please note that RMSE for each feature is calculated as the difference between the ground truth and the measured feature using different current levels, U and activity state X and each value is squared. We then square each difference to get a positive value, find the summation over each time period, divide the result by the length of the calculated feature, and calculate the root of it. The variables $\gamma_1, \gamma_2, \gamma_3$ are normalized weights corresponding to each feature, with $0 < \gamma_1 \leq \gamma_2 \leq \gamma_3 < 1$. The control parameter U specifies the PPG sensor's current level. The block diagram of system design-time is shown in Figure 12.

Optimization Problem: In this method, the energy consumption in the sensor $E(U,X)$ is a function of the patient's activity and sensor's current level. Note that error measurements of the sensor $\epsilon(U,X)$ as a function of the patient's activity and sensor's current level should satisfy a desired threshold τ. Therefore, the sensing fidelity is selected to minimize energy expense under a constraint on the minimum accuracy in terms of overall RMSE. Thus,

$$\min_{U} E(U,X) \text{ subject to } \epsilon(U,X) \leq \tau \tag{3}$$

The defined formulation is a convex optimization problem where one optimal solution can be obtained. Lagrangian function $\mathcal{L}(U,\lambda)$ is defined as a function of Lagrangian multiplier λ and current level U to solve the optimization problem,

$$\mathcal{L}(U,\lambda) = E(U,X) + \lambda(\epsilon(U,X) - \tau) \tag{4}$$

where, λ is the trade-off parameter determining the relative importance of RMSE and the Energy cost. The goal is to select the variable U for each activity level X such that the total cost will be minimized. Therefore, we take the derivative of the Lagrangian function with respect to the sensor's current level,

$$\frac{\partial E(U,X)}{\partial U} + \lambda \frac{\partial \epsilon(U,X)}{\partial U} = 0 \tag{5}$$

Considering a linear relation between energy consumption and sensor's current level, derivative of $E(U,X)$ with respect to U is a constant value a_U. The total RMSE $\epsilon(U,X)$ can be interpolated as a linear combination of the current level U. The derivative of $\epsilon(U,X)$ with respect to U will be a constant value b_U. Therefore, the Lagrangian multiplier can be calculated as $\lambda = -\frac{b_U}{a_U}$. Solving this optimization problem will obtain the optimal current level U^*. Using this optimization solution, we developed the *Sensing Fidelity Run-time* to determine the optimal current level in the monitoring.

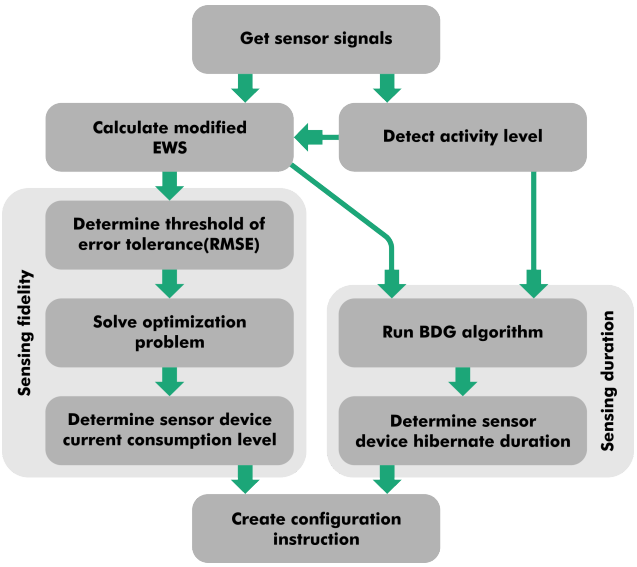

Fig. 13. The readjustment algorithm

ii) Sensing Fidelity Run-time: In this phase, the edge processor periodically determines the lowest sensor's current level in real-time such that the total RMSE of the extracted features is less than a desired threshold.

4.2.2 Sensing and Hibernation Duration. To adjust the sensing device parameters, we consider a state machine which consists of four states for the patient and five states for the device. We define two states for patient health status according to the EWS score [35], where any score below 3 is considered as normal conditions (H1), and scores equal or above 3 as abnormal condition (H2). Similarly, we consider sleeping and walking as low-intensity activities (A1) and walking, jogging, and running as high-intensity activities (A2). Recent work has shown that five minutes is a reasonable interval to capture changes in one's activity [51]. Therefore, we set the sensing duration to five minutes and five different duration for hibernation from m1 to m5 minutes. Since we aim to capture the states changing moment, the hibernation time is preferred to be elongated as long as no change happens to the patient health or activity status. The sensing device follows the state machine shown in Figure 14. It starts with state S1, which has the longest hibernation time and stays there as long as no adverse event happens. With any abnormal or intense activity event, it switches to the state S5, which has the lowest hibernation time (i.e., zero hibernation time or continuous monitoring) and stays there while the abnormality is there. When the patient faces the normal condition again, it increases the hibernation time step by step by switching to other states from S4 to S1. The device does not stay in S4 to S2 states and just passes them one by one to reach the initial state. It is a reasonable decision since the abnormality may return again, and the health re-assessment of the patient would be possible with the shortest delay.

5 DEMONSTRATION AND EVALUATION

A remote reconfigurable sensor node was implemented together with the required edge services to collect vital signs, assess the accuracy of sensors in different modes, and evaluate the energy efficiency of the system. A system for collecting the baseline for each parameter of interest was

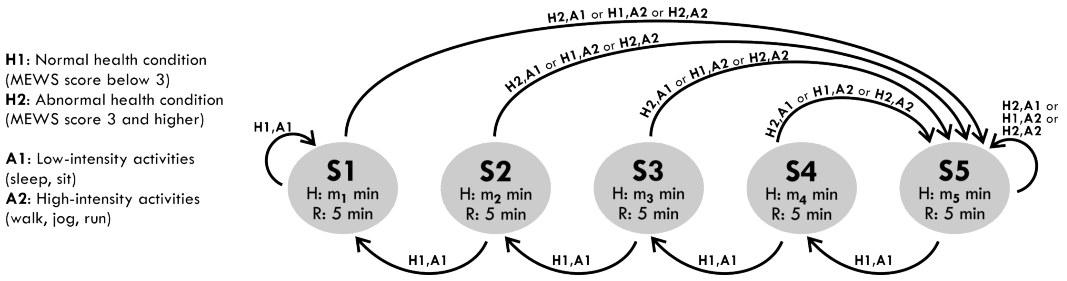

Fig. 14. Sensing device readjustment state machine

also designed. We use ESP8266-12E WiFi module as a core for the sensor node. This module has an 80MHz 32-Bits RISC microprocessor with 96KB RAM and 4MB QSPI flash memory. Three sensor modules are connected to this core, all of which are digital sensors configurable by internal registers via I^2C communication. The primary sensor module is MAX30102 PPG sensor placed on the left hand index fingertip. This module has two LEDs and a light sensor working in 880nm wavelength (infrared) and 660nm wavelength (red). The sampling rate and the current level of LEDs (and thus their brightness) are configurable. The current level for driving the LEDs in the PPG sensor can be configured to be one of the 0.8mA, 3.5mA, 6.3mA, 9.2mA or 12mA values. Other sensors are TEMP102 temperature sensor module and MMA8451 3D accelerometer sensor module attached to the left hand palm.

Figure 15 shows the sensor node. Since the fingertip is the most common site for PPG measurement [66], we collected our reference signals from the fingertip and designed the sensing device to record the PPG signal from this site on left hand index finger. The wearable device is in the form of a glove which contains the electronic circuit and covers the sensor to prevent ambient light from interfering with it. The user is expected to wear the glove during the monitoring. Compare to other potential solutions for measuring the EWS, which requires a chest strap for heart rate, a respiration sensor on the nostril, and a grip on finger or ear for SpO_2, this glove-shaped sensing device is very compact and easy-to-wear. Since the sensor node uses Wi-Fi communication for data transmission, the gateway should be a portable device. Therefore, we use an Android phone as a gateway in our experiments. We implement the readjustment algorithm on the phone using the Python programming language. A Samsung S6 Android phone with 1.5GHz octa-core processor and 3GB RAM acts as a hotspot and creates a wireless network. It uses QPython script engine [62] to create a web server and run the Python readjustment code. The cloud server is a virtual private server (VPS) running an Apache web server and Python on an Ubuntu OS to perform periodic RMSE updates.

The web service on the gateway device responds to configuration requests and performs the readjustment algorithm for setting the sensor node configuration. The sensor node has three states: recording state, transmission state, and hibernate state. According to the configuration, the recording state has its own sub-states. We measure the power consumption of each state using a power monitor device. Table 2 shows sensor node power consumption in each state.

5.1 Accuracy Assessment

In this section, the performance of the proposed system is evaluated in terms of accuracy. We conduct 12.5 hours of experiments including 150 ($6 \times 5 \times 5$) different conditions where six healthy users engage five different activities (i.e., Sleeping, Sitting, Walking, Jogging and Running) and the PPG sensor varies as a function of current (i.e., 0.8mA, 3.5mA, 6.3mA, 9.2mA and 12mA).

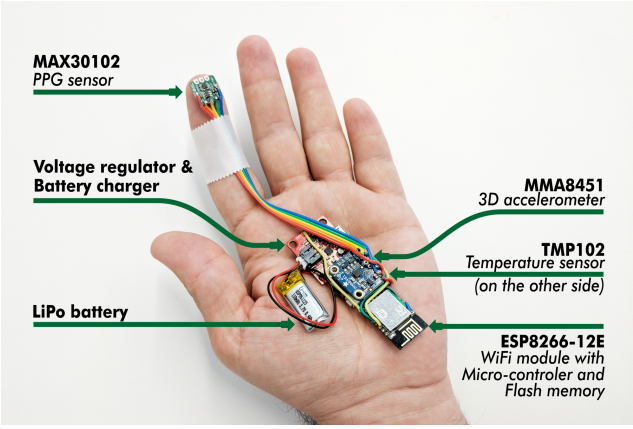

Fig. 15. Sensor node and its components

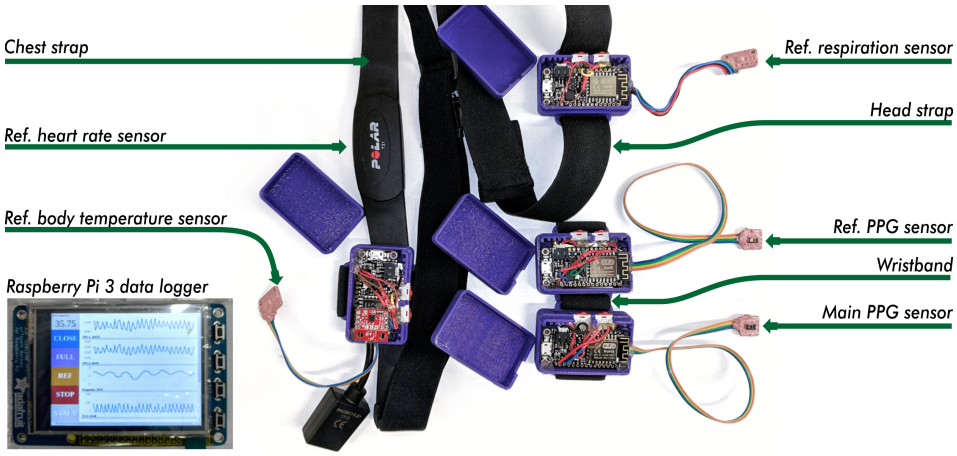

Fig. 16. Reference signals wireless data logger

For each activity type, data collection was performed for 5 minutes. 30-second interval time was selected as a computation window to extract vital signs from the PPG signal. Therefore, 10 values are obtained for each activity. To collect the assessment reference signals, we develop a wireless vital sign data logger which consists of four sensor nodes. The sensor nodes are developed using Adafriut HUZZAH which is a development board for ESP8266-12E WiFi module. The recording device is a Raspberry Pi 3 board equipped with a 3.5in display hat that records data and displays the signals in real-time. A NodeJS server on the Raspberry Pi 3 board is responsible for receiving data samples via UDP packets and recording them on the MicroSD card. Figure 16 shows the sensor nodes and the Raspberry Pi 3 data logger. In this setup:

- A wristband fixes two nodes on the left wrist that record the main PPG signal from the index finger's tip and reference PPG signal from the middle finger's tip.

- A head strap fixes a node on the forehead and a very accurate and sensitive temperature sensor (MCP9808) sits in front of the nostril to sense the real respiration signal. The sensor gets warm

State	Sensor node power consumption
R1: Recording, LEDs setting: 0.8mA	69.30 mW
R2: Recording, LEDs setting: 3.5mA	73.26 mW
R3: Recording, LEDs setting: 6.3mA	79.86 mW
R4: Recording, LEDs setting: 9.2mA	84.15 mW
R5: Recording, LEDs setting: 12mA	89.43 mW
T: Transferring	244.2 mW
H: Hibernate	5.94 mW

Table 2. Sensor node states power consumption

	Hibernation Time (Minute)					Total Recording Time (% of the day)	Total Missing Events (%)	Average Power Consumption (mW)
	m1	m2	m3	m4	m5			
Scenario 1	16	12	8	4	0	28.7%	30%	39.2mW
Scenario 2	8	6	4	2	0	41.1%	20%	53.8mW
Scenario 3	8	4	2	1	0	41.5%	10%	54.2mW
Scenario 4	7	5	3	1	0	44.6%	0	58mW
Scenario 5	4	3	2	1	0	57.8%	0	69.5mW
Baseline	0	0	0	0	0	83.3%	0	115.2mW

Table 3. Total monitoring time, average power consumption, and missing event due to different scenarios for sensing device hibernation duration

during the exhale and gets cold during the inhale. The result is an oscillating signal which we use to calculate the respiration rate reference.

- The 4th sensor node utilizes an ECG measurement chest strap (Polar T31) as a reference for the real heart rate. It also contains a body temperature sensor (TMP102) and a 3D-accelerometer sensor (MPU-9250).

To assess the accuracy, the extracted values through the PPG sensor are compared with the true values. The total RMSE is calculated (see Section 4.2.1) to determine errors in the monitoring with different user's activities and different PPG sensor's current level. As illustrated in Figure 17, the error increases when (a) the the amount of activity increases, and (b) the sensing current decreases. This is more significant in case of vigorous activities. 3.5mA is the boundary (i.e., lowest current level) where an acceptable result could be obtained in any physical activity. However, this boundary is 6.3mA for running and jogging activities. We tailor such information for our cognitive edge controller design to deliver a satisfactory outcome, ensuring that the RMSE does not exceed the threshold through the monitoring process. In the proposed architecture, the procedure of calculating RMSE happens on the cloud server and its periodic recalculation requires collecting new reference data that can be performed when the patient is ready to repeat the reference signals data collection procedure.

5.2 Energy Evaluation

Energy management in the edge layer is an important factor to control the limited resources in the sensor layer. To evaluate the proposed state machine in Sections 4.2 and 4.2.2, a healthy individual was monitored during a 24-hour activity using the proposed sensor layer and controller in the edge with different sets of timings for hibernation. We defined these timings in our state machine as m_1,

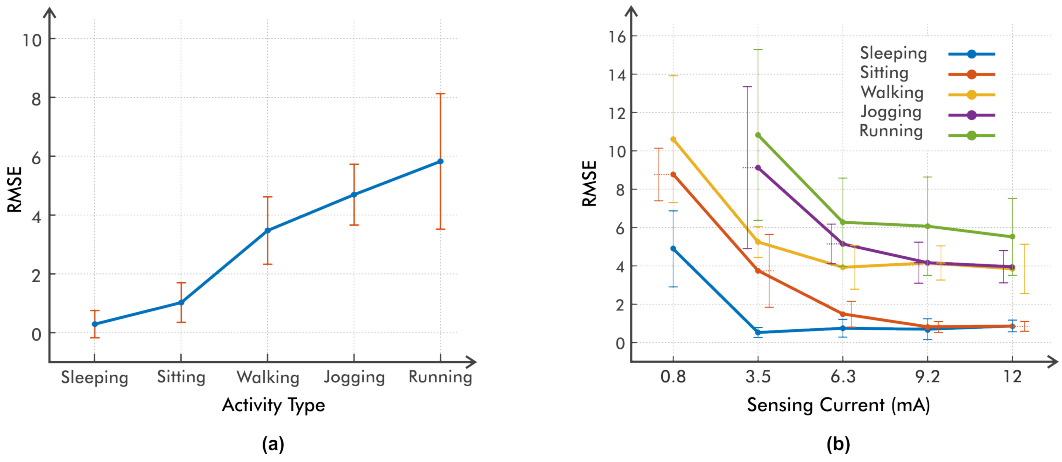

Fig. 17. (a) The effect of activity type on total RMSE, (b) The average of total RMSE for heart rate, respiration rate and SpO_2 in different activities

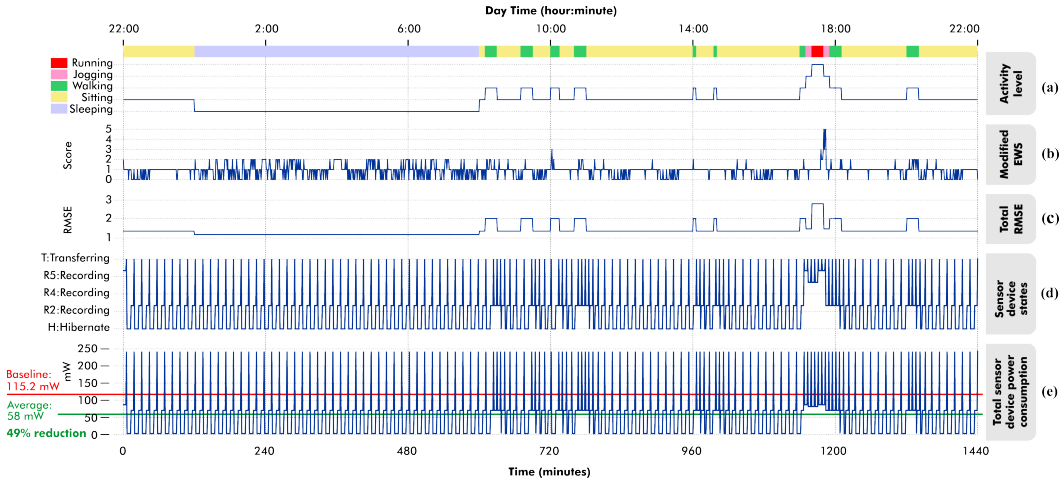

Fig. 18. 24-hours health monitoring of a healthy person. (a) user's activity level. (b) calculated modified EWS. (c) sensor's current level. (d) total RMSE expected regarding the user's activity. (e) device states including hibernate, different recordings and data transferring. (f) device power consumption through the monitoring. The red line and green line indicate the baseline and our proposed system power consumption, respectively.

m_2, m_3, m_4, and m_5. Definitely, using higher values for hibernation duration leads to lower energy consumption, but with longer hibernation, some of the important health or activity events that happen during the hibernation may be missed. To find an optimal set of timings we define five different scenarios and assess the energy efficiency of the sensing device in each scenario. Table 3 shows the timing of each scenario, the total daily monitoring time, the percentage of missing events, and the average power consumption of the sensing device. We choose the 4th scenario which is the most efficient one without missing events. Recording the PPG signal and body temperature in the sensor layer along with the activity level in the edge layer, we calculated the modified EWS score from the extracted vital signs. Figures 18 (a) and 18 (b) demonstrate the activity level and calculated

EWS score. By extracting the EWS score and activity level, the readjusting algorithm is executed. At each given time, based on the EWS score and activity level, the threshold of RMSE will be determined. High-level activities and/or high EWS score necessitate accurate monitoring leading to choosing lower RMSE threshold values. In contrast, low-level activities including, "Sitting" and "Sleeping" with normal EWS score can tolerate some higher threshold of total RMSE.

In this experiment, we considered high-level activities and/or high EWS score that can tolerate at maximum 1 in error in HR, maximum of 1 error in RR and maximum of 0.5 error in SpO_2. The parameters defining the total RMSE are chosen based on the sensitivity of each vital signs during different activities. Oxygen saturation has high sensitivity compared to other features in lower current levels and can hardly be detected in low current levels due to mitigation of noise in the signal. Respiratory rate is less sensitive to noise compared to the oxygen saturation. However, the respiration rate is more prone to noise compared to the heart rate. Therefore, the three parameters $\gamma_1, \gamma_2, \gamma_3$ are chosen based on the variations of the vital signs, so features with more sensitivity have a slightly higher impact on calculating $RMSE$ to take the sensitivity into account. Therefore, the total RMSE threshold will be $\tau = \gamma_1\epsilon_1 + \gamma_2\epsilon_2 + \gamma_3\epsilon_3$ for $\gamma_1 < \gamma_2 < \gamma_3$ and $\gamma_1 + \gamma_2 + \gamma_3 = 1$ (described in Section 4.2). This leads to a threshold of $\tau = 0.25 \times 1 + 0.35 \times 1 + 0.4 \times 0.5 = 0.8$. Low level activities with normal EWS score can tolerate an error of $\epsilon_1 = 2$, $\epsilon_2 = 2$ and $\epsilon_3 = 1$. The threshold for RMSE will be $\tau = 0.25 \times 2 + 0.35 \times 2 + 0.4 \times 1 = 1.6$. At each given time, the edge layer chooses the lowest sensor's current level to satisfy the threshold τ given the activity and EWS score calculation of an individual. Figure 18 (c) determines the total RMSE that is expected by choosing each current level. Note that the lowest RMSE values that can be obtained during "Running" and "Jogging" states are 2.931 and 1.431, respectively. In other words, due to motion artifacts, even the maximum current level cannot improve the accuracy over a certain threshold. The average RMSE observed during the experiment was 1.3276. Figure 18 (d) illustrates the implementation of the state machine while running the scenario 4 for hibernation timings, determining the time the sensor toggles between the on/transmit/off states. At each given time, when the sensor is on, detection of high-level activity and/or high EWS score resets the hibernating time of the sensor to zero. Lower level activities with normal EWS score enables the sensor node hibernation duration to increase state by state. Figure 18 (e) shows the total power consumption of the sensor taking account the system state and sensing duration. The average total power consumption in this experiment was recorded to be 58 mW. Considering monitoring an individual with constant 12 mA sensor's current level for 24 hours in 5-minutes intervals (i.e., the baseline) 115.2 mW power consumption in the sensor node can be obtained. Consequently, we observe that the edge controller is able to save 49% of the battery power for this case study, demonstrating the efficacy of our edge-assisted intelligent control scheme.

6 CONCLUSIONS

IoT technology and edge computing create new avenues for health monitoring and enable the delivery of desirable Quality of Experience (QoE) to patients and healthcare providers in the face of resource constraints and dynamic user behavior. In this context, traditional schemes have investigated the optimization of system-driven and data-driven aspects separately, resulting in missed opportunities for better optimization and system responsiveness to meet dynamically changing healthcare application scenarios. In this paper, we outlined a scheme that jointly combines system-driven and data-driven aspects using cognitive edge-assisted control, to deliver desirable QoE while saving precious energy resources.

We presented a case study that deploys an edge-based health monitoring system that adjusts itself to the most energy-efficient setting while retaining a desirable level of accuracy, considering patient

medical and activity state. We implemented our optimization method and run-time algorithm on a reconfigurable sensor node and assessed the efficiency of our proposed system through a PPG-based Early Warning Score system case study. We demonstrated that our proposed edge-assisted system reduced 49% of the overall power consumption by adapting to patient health state and activity level while assuring a minimum level of accuracy. This scale provides a vision that a context-aware system will consume approximately half of the energy that a non-context-aware system uses to provide the same service. In the future work, we will optimize data transfer bandwidth considering sensor selection and sensing sampling rate w.r.t. the patient's conditions during the monitoring.

ACKNOWLEDGEMENTS

This work was partially supported by the US National Science Foundation (NSF) WiFiUS grant CNS-1702950 and Academy of Finland grants 311764 and 311765.

REFERENCES

[1] A. Aijaz et al. Cognitive machine-to-machine communications for internet of things: A protocol stack perspective. *IEEE Internet of Things*, 2:103–112, 2015.
[2] J. Allen. Photoplethysmography and its application in clinical physiological measurement. *Physiol Meas.*, 28(3):1–39, 2007.
[3] D. Amiri et al. Edge-assisted sensor control in healthcare iot. In *GLOBECOM'18 Conf.*, pages 1–6, 2018.
[4] D. Amiri et al. Context-aware sensing via dynamic programming for edge-assisted wearable systems. *ACM Trans. Comput. Healthcare*, 1(2), 2020.
[5] D. Amiri et al. *Optimizing Energy Efficiency of Wearable Sensors Using Fog-assisted Control*, chapter 9, pages 245–268. John Wiley and Sons, Ltd, 2020.
[6] D. Anguita et al. Energy efficient smartphone-based activity recognition using fixed-point arithmetic. *J. UCS*, 19(9):1295–1314, 2013.
[7] A. Anzanpour et al. Internet of things enabled in-home health monitoring system using early warning score. In *MobiHealth'15 Conf.*, 2015.
[8] A. Anzanpour et al. Context-aware early warning system for in-home healthcare using internet-of-things. In *HealthyIoT'16 Conf.*, 2016.
[9] A. Anzanpour et al. Self-awareness in remote health monitoring systems using wearable electronics. In *DATE'17 Conf.*, 2017.
[10] A. Anzanpour et al. Energy-efficient and reliable wearable internet-of-things through fog-assisted dynamic goal management. In *ANT'19 Conf.*, 2019.
[11] I. Azimi et al. Self-aware early warning score system for iot-based personalized healthcare. In *LNICST'16 Conf.*, 2016.
[12] K. Bartels et al. Advances in photoplethysmography: beyond arterial oxygen saturation. *Canadian Journal of Anaesthesia*, 62(12):1313–1328, 2015.
[13] F. Bonomi et al. Fog computing and its role in the internet of things. In *First Edition of the MCC Workshop on Mobile Cloud Computing*, pages 13–16, 2012.
[14] F. Bonomi et al. Fog computing: A platform for internet of things and analytics, in big data and internet of things: A roadmap for smart environments. In *Big Data and Internet of Things*, 2014.
[15] M. Brabrand et al. Risk scoring systems for adults admitted to the emergency department: a systematic review. *SJTREM*, 18:8, 2010.
[16] P. C.-P. Chao et al. A portable, wireless photoplethysomography sensor for assessing health of arteriovenous fistula using class-weighted support vector machine. *Sensors (Basel)*, 18, 2018.
[17] P. Charlton et al. An assessment of algorithms to estimate respiratory rate from the electrocardiogram and photoplethysmogram. *Physiol Meas.*, 37(4):610–26, 2016.
[18] B.-G. Chun et al. Clonecloud: Elastic execution between mobile device and cloud. In *EuroSys'11 Conf.*, 2011.
[19] E. Cuervo et al. Maui: Making smartphones last longer with code offoad. In *MobiSys'10 Conf.*, pages 49–62, 2010.
[20] O. Dur et al. Design rationale and performance evaluation of the wavelet health wristband: Benchtop validation of a wrist-worn physiological signal recorder. *JMIR Mhealth Uhealth*, 6, 2018.
[21] A. Garde et al. Estimating respiratory and heart rates from the correntropy spectral density of the photoplethysmogram. *PLoS One*, 9(1), 2014.
[22] D. Gordon et al. Energy-efficient activity recognition using prediction. In *ISWC'12 Conf.*, 2012.

[23] W. B. Gratzer. . Med. Res. Council Labs, Holly Hill, London.
[24] M. Götzinger et al. Enhancing the self-aware early warning score system through fuzzified data reliability assessment. In *MobiHealth'17 Conf.*, 2017.
[25] M. Götzinger et al. Confidence-enhanced early warning score based on fuzzy logic. *ACM/Springer Mobile Networks and Application*, 2019.
[26] K. Ha et al. Towards wearable cognitive assistance. In *MobiSys'14 Conf.*, pages 68–81, 2014.
[27] J. Hendrikx et al. Clinical evaluation of the measurement performance of the philips health watch: A within-person comparative study. *JMIR Mhealth Uhealth*, 2(5), 2017.
[28] A. Hertzman. The blood supply of various skin areas as estimated by the photoelectric plethysmograph. *American Journal of Physiology*, 124:328–340, 1938.
[29] C. M. Hsieh et al. Dance: Distributed application-aware node configuration engine in shared reconfigurable sensor networks. In *DATE'13 Conf.*, 2013.
[30] P. Hu et al. Fog computing based face identification and resolution scheme in internet of things. *IEEE Trans. Ind. Inform.*, 13(4):1910–1920, 2017.
[31] M. Integrated. , (accessed 2018-08-01). https://www.maximintegrated.com/en/products/sensors/MAX30102.html.
[32] B. M. Jayadevappa et al. Photoplethysmography: Design, development, analysis and applications in clinical and physiological measurement – a review. *IJIRSET*, 5(3):3519–3531, 2016.
[33] W. Karlen et al. Multiparameter respiratory rate estimation from the photoplethysmogram. *IEEE Trans. on Biomedical Engineering*, 60(7):1946–53, 2013.
[34] N. Kollias. . Wellman Lab, Harvard Medical School, Boston.
[35] U. Kyriacos et al. Monitoring vital signs: development of a modified early warning scoring (mews) system for general wards in a developing country. *PloS one*, 9(1), 2014.
[36] X. S. Le et al. Cardin: An agile environment for edge computing on reconfigurable sensor networks. In *CSCI'16 Conf.*, 2016.
[37] R. LiKamWa et al. Energy characterization and optimization of image sensing toward continuous mobile vision. In *MobiSys'13 Conf.*, pages 69–82, 2013.
[38] L. G. Lindberg et al. Monitoring of respiratory and heart rates using a fibre-optic sensor. *Med. Biol. Eng. Comput.*, 30(5):533–7, 1992.
[39] J. Ludikhuize et al. Identification of deteriorating patients on general wards; measurement of vital parameters and potential effectiveness of the modified early warning score. *J. Crit. Care.*, 27(4), 2012.
[40] L. A. Lynn and J. P. Curry. Patterns of unexpected in-hospital deaths: a root cause analysis. *Patient Safety in Surgery*, 5(1), 2011.
[41] I. D. Mapp et al. Predicting clinical deterioration in the hospital: the impact of outcome selection. *Resuscitation*, 84(5), 2013.
[42] I. D. Mapp et al. Prevention of unplanned intensive care unit admissions and hospital mortality by early warning systems. *Dimens Crit Care Nurs.*, 32(6), 2013.
[43] Y. O. Mohammed and U. A. Baroudi. Partially observable markov decision processes (pomdps) and wireless body area networks (wban): A survey. *KSII Trans. on Internet and Information Systems*, 7, 2013.
[44] J. Moody et al. A -76dbm 7.4nw wakeup radio with automatic offset compensation. In *ISSCC'18 Conf.*, 2018.
[45] R. Morgan et al. An early warning scoring system for detecting developing critical illness. *Clin Intensive Care*, 8:100, 1997.
[46] E. K. Naeini et al. An edge-assisted and smart system for real-time pain monitoring. In *CHASE'19 Conf.*, pages 47–52, 2019.
[47] E. K. Naeini et al. A real-time ppg quality assessment approach for healthcare internet-of-things. *Procedia Computer Science*, 151:551–558, 2019.
[48] S. Natheswaran and G. Athisha. Remote reconfigurable wireless sensor node design for wireless sensor network. In *ICCSP'14 Conf.*, 2014.
[49] B. Nelson and N. Allen. Accuracy of consumer wearable heart rate measurement during an ecologically valid 24-hour period: Intraindividual validation study. *JMIR Mhealth Uhealth*, 7(3), 2019.
[50] T. Nyländen et al. Reconfigurable miniature sensor nodes for condition monitoring. In *SAMOS'12 Conf.*, 2012.
[51] H. Oh and R. Jain. From multimedia logs to personal chronicles. In *MM'17 Conf.*, 2017.
[52] C. O'Keeffe et al. Role of ambulance response times in the survival of patients with out-of-hospital cardiac arrest. *Emerg Med J.*, 28(8):703–6, 2011.
[53] P. Patel et al. On using the intelligent edge for iot analytics. *IEEE Intelligent Systems*, 32(5):64–69, 2017.
[54] M. A. F. Pimentel et al. *Probabilistic Estimation of Respiratory Rate from Wearable Sensors*, pages 241–62. Springer, 2015.
[55] M. R. Ra et al. Odessa: Enabling interactive perception applications on mobile devices. In *MobiSys'11 Conf.*, pages 43–56, 2011.

[56] A. M. Rahmani et al. *Fog Computing in the Internet of Things - Intelligence at the Edge.* Springer, 2017.
[57] A. M. Rahmani et al. Exploiting smart e-health gateways at the edge of healthcare internet-of-things: a fog computing approach. *Future Generation Computer Systems*, 78(2):641–58, 2018.
[58] R. K. Reddy et al. Accuracy of wrist-worn activity monitors during common daily physical activities and types of structured exercise: Evaluation study. *JMIR Mhealth Uhealth*, 6(12), 2018.
[59] S. Sarkar and S. Misra. Theoretical modelling of fog computing: a green computing paradigm to support iot applications. *IET Netw.*, 5(2):23–29, 2016.
[60] S. Sasidharan et al. Cognitive management framework for internet of things: x2014; a prototype implementation. In *WF-IoT'14 Forum*, pages 538–543, 2014.
[61] M. Satyanarayanan et al. Edge analytics in the internet of things. *IEEE Pervasive Computing*, 14:24–31, 2015.
[62] Q. scripting engine. , (accessed 2018-08-01). https://www.qpython.com/.
[63] A. Sheth. Internet of things to smart iot through semantic, cognitive, and perceptual computing. *IEEE Intelligent Systems*, 31(2):108–112, 2016.
[64] D.-H. Shin. Conceptualizing and measuring quality of experience of the internet of things: Exploring how quality is perceived by users. *Information & Management*, 54:998–1011, 2017.
[65] A. Taenzer et al. A review of current and emerging approaches to address failure-to-rescue. *Anesthesiology*, 115(2):421–431, 2011.
[66] T. Tamura et al. Wearable photoplethysmographic sensors—past and present. *Electronics*, 3:282–302, 2014.
[67] G. B. Tayeh et al. A new autonomous data transmission reduction method for wireless sensors networks. In *MENACOMM'18 Conf.*, 2018.
[68] TeleTracking. The value of time in healthcare. *White paper*, 2004.
[69] J. Tervonen et al. Cognitive internet-of-things solutions enabled by wireless sensor and actuator networks. In *CogInfoCom'14 Conf.*, pages 97–102, 2014.
[70] V. Toral et al. Reconfigurable ppg: Wearable system for biosignal acquisition and monitoring based on reconfigurable technologies. *Sensors (Basel)*, 19, 2019.
[71] C. Tudor-Locke et al. Pedometer-determined step count guidelines for classifying walking intensity in a young ostensibly healthy population. *Can J Appl Physiol.*, 30(6):666–76, 2005.
[72] C. Tudor-Locke et al. Patterns of adult stepping cadence in the 2005-2006 nhanes. *Prev Med.*, 53(3):178–81, 2011.
[73] R. W. Urban et al. Modified early warning system as a predictor for hospital admissions and previous visits in emergency departments. *Advanced emergency nursing journal*, 37(4):281–289, 2015.
[74] Y. Wang et al. A framework of energy efficient mobile sensing for automatic user state recognition. In *Mobisys'09 Conf.*, 2009.
[75] M. Weenk et al. Continuous monitoring of vital signs using wearable devices on the general ward: Pilot study. *JMIR Mhealth Uhealth.*, 5(7), 2017.
[76] Q. Wu et al. Cognitive internet of things: A new paradigm beyond connection. *IEEE Internet of Things Journal*, 1:129–143, 2014.
[77] M. P. Young et al. Inpatient transfers to the intensive care unit: delays are associated with increased mortality and morbidity. *J Gen Intern Med.*, 18:77–83, 2003.
[78] D. S. Zois et al. A pomdp framework for heterogeneous sensor selection in wireless body area networks. In *INFOCOM'12 Conf.*, pages 2611–5, 2012.
[79] D. S. Zois et al. Energy-efficient, heterogeneous sensor selection for physical activity detection in wireless body area networks. *IEEE Trans. signal processing*, 61(7):1581–94, 2013.
[80] D. S. Zois et al. Active classification for pomdps: A kalman-like state estimator. *IEEE Trans. on Signal Processing*, 62(23):6209–24, 2014.